

## A facile synthesis of cysteine- ferrite magnetic nanoparticles for application in multicomponent reactions– A sustainable protocol

Manoj B. Gawande,<sup>\*a</sup> Paula S. Branco,<sup>\*a</sup> Alexandre Velhinho,<sup>b</sup> Isabel D. Nogueira,<sup>c</sup> C. A. A. Ghumman,<sup>d</sup> O.M.N.D. Teodoro<sup>d</sup>

<sup>a</sup> REQUIMTE, Departamento de Química, Faculdade de Ciências e Tecnologia, FCT, Universidade Nova de Lisboa, 2829-516 Caparica, Portugal Fax: +351 21 2948550; Tel: +351 21 2948300. Email: [mbgawande@yahoo.co.in](mailto:mbgawande@yahoo.co.in), [m.gawande@fct.unl.pt](mailto:m.gawande@fct.unl.pt) (Dr. Manoj Gawande); [paula.branco@fct.unl.pt](mailto:paula.branco@fct.unl.pt) (Prof. Paula S. Branco)

<sup>b</sup> CENIMAT/I3N Departamento de Ciências dos Materiais, Faculdade de Ciências e Tecnologia, FCT, Universidade Nova de Lisboa, 2829-516 Caparica, Portugal

<sup>c</sup> Instituto de Ciência e Engenharia de Materiais e Superfícies, IST, Lisbon, Portugal

<sup>d</sup> Centre for Physics and Technological Research (CeFITec), Departamento de Física da Faculdade de Ciências e Tecnologia (FCT), Universidade Nova de Lisboa, 2829–516 Caparica, Portugal

General methods and experimental procedures	2
Preparation of ferrites and ferrite-Cys MNPs	3
Synthesis of $\beta$ -Amino ( <b>3</b> )	3
Optimization of reaction conditions with benzaldehyde ( <b>5a</b> ) and aniline ( <b>4a</b> )	4
Síntese of hexahydro-quinoline derivative ( <b>7</b> )	6
FT-IR of Ferrite, L-Cysteine and Ferrite-Cys	7
TOF-SIMS analysis of Ferrite-Cys	8
Field-emission gun scanning electron microscope (FEG-SEM)	10
Transmission electron microscopy (TEM) of Ferrite-Cys	11
Stability of Ferrite-Cys	13
References	15
NMR Spectrum of compounds	16

## General methods and experimental procedures

All commercial reagents were used as received unless otherwise mentioned. For analytical and preparative thin-layer chromatography, Merck, 0.2 mm and 0.5 mm Kieselgel GF 254 percoated were used, respectively. The spots were visualized using UV light.

The X-ray powder diffraction pattern was obtained using a conventional powder diffractometer RIGAKU, model: MiniFlex™ II benchtop X-ray Diffractometer; X-ray tube: Cu-K $\alpha$  (30 kV / 15 mA) radiation operating in Bragg-Brentano ( $\theta/2\theta$ ) geometry. (Sample preparation: grinding when needed and compression in the sample holder with a flat glass. The sample area in the sample holder is about 2 cm<sup>2</sup>). Transmission electron microscopy (TEM) experiments were performed on a Hitachi H8100 microscope, with a ThermoNoran light elements EDS detector and a CCD camera for image acquisition. The Fe<sub>3</sub>O<sub>4</sub>-Cys fine powder was placed on carbon stub and the images were recorded at 5-15 kV using LFD detector under low vacuum.

Elemental analysis was done by using ICP-AES (Inductively coupled plasma-atomic emission spectrometer) using a Horiba Jobin-Yvon, France, Ultima, model equipped with a 40.68 MHz RF generator, Czerny-Turner monochromator with 1.00 m (sequential), autosampler AS500 and CMA (concomitant metals analyzer).

Scanning electron microscopy images were acquired using a JEOL JSM7001F FEG-SEM. Elemental analysis was performed using light elements EDS detector from Oxford. The ferrite-cysteine powder was spread on a double-sided carbon tape and analyzed using 25 kV acceleration voltage.

For SIMS, (secondary ion mass spectrometry) positive and negative secondary ion spectra were collected in the mass range of 0.5-500  $m/z$  (T=10 min) with an upgraded VG Ionex IX23LS TOF-SIMS set-up based on the Poschenrieder design. A focused liquid Ga<sup>+</sup> gun in pulsed mode (6 kHz) was used as a source of the analytical ions. A beam current in dc mode at 14 keV was ca. 15 nA with a raster size of 300 X 300  $\mu\text{m}^2$ . Sample potential was 5 kV. Vacuum during the experiments was maintained in the range of (2-3) X10<sup>-9</sup> mbar in the analytical chamber.

Infrared spectra were recorded on a Perkin Elmer spectrum 1000. <sup>1</sup>H NMR spectra were recorded on a Bruker ARX400 spectrometer at 400 MHz. <sup>1</sup>H shifts are reported relative to

internal TMS. Mass spectra were recorded at the Mass Spectrometry Unit at the University of Santiago de Compostela, Spain using a magnetic Micromass Autospec apparatus.

### **Preparation of ferrites and ferrite-Cys MNPs**

#### **Preparation of Ferrites /Fe<sub>3</sub>O<sub>4</sub>**

The FeCl<sub>3</sub>.6H<sub>2</sub>O (5.4 g) and urea (3.6 g) were dissolved in water (200 mL) at 85 to 90 °C for 2 h. The solution turned brown in color. The resultant reaction mixture was cooled to room temperature to which was added FeSO<sub>4</sub>.7H<sub>2</sub>O (2.8 g) and then 0.1 M NaOH until pH 10. The molar ratio of Fe (III) to Fe (II) in the above system was nearly 2.00. The obtained hydroxides were treated by ultrasound in the sealed flask at 30 to 35 °C for 30 min. After ageing for 5 h the obtained black powder of Fe<sub>3</sub>O<sub>4</sub> was washed, and dried under vacuum.

#### **Preparation of Fe<sub>3</sub>O<sub>4</sub>-cysteine**

Fe<sub>3</sub>O<sub>4</sub> MNPs (1 gm) were dispersed in 20 mL of distilled water and L-cysteine (1 g) dissolved in 40-50 mL of methanol:water (1:1) was added to the dispersed ferrite MNPs and the reaction mixture stirred at room temperature for 24 h (1200 RPM) using a magnetic stirrer device. The Fe<sub>3</sub>O<sub>4</sub>-Cys MNPs was then isolated by simple magnetic decantation and successively washed with water (2 X 10 mL) and methanol (2 X 10 mL) and dried under vacuum at 60 °C for 2 h.

### **Synthesis of β-Amino ketones (3)**

A mixture of benzaldehyde (5.0 mmol), aniline (5.0 mmol), cyclohexanone (10 mmol), and Fe<sub>3</sub>O<sub>4</sub>-Cys (5 wt % respectively to aldehyde) was stirred under solvent-free conditions at room temperature for an appropriate time. After completion of reactions monitored by TLC (n-hexane and ethyl acetate; 70:30), 10 mL of ethyl acetate was added to the reaction mixture and the catalyst separated magnetically. The organic layer was washed with saturated NaHCO<sub>3</sub>(aq) and brine, dried with anhydrous Na<sub>2</sub>SO<sub>4</sub> and concentrated to dryness. The crude mixture was purified by crystallization in ethanol or if necessary subjected to flash column chromatography.

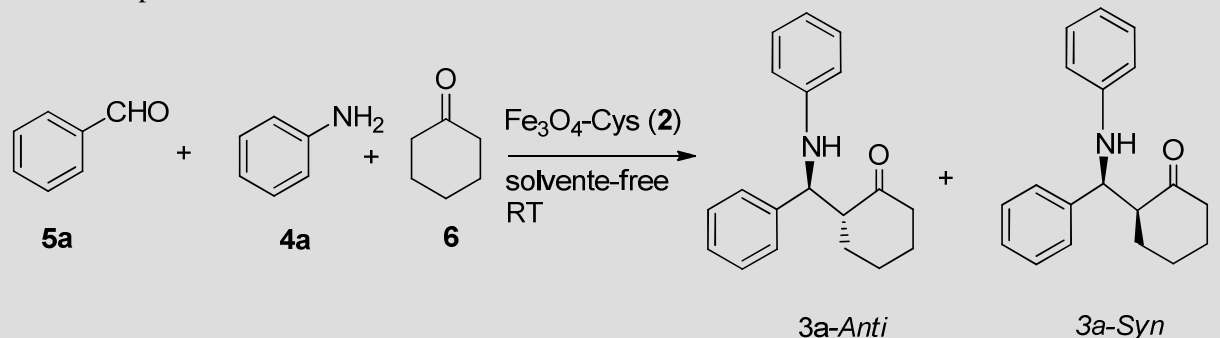
### Optimization of reaction conditions with benzaldehyde (**5a**) and aniline (**4a**).

The model reaction between benzaldehyde and aniline was conducted in various solvents at 22°C (Table 1) and the  $\beta$ -amino-ketone **3a** was obtained in moderate to high yields. The best results were observed in solvent-free conditions (Table 1, entry 7). Under solvent- and catalyst free conditions, only trace amounts of the  $\beta$ -amino-ketone **3a** were observed (Table 1, entry 1) along with the imine that result from the condensation of benzaldehyde and aniline. Moderate to high selectivity was observed in polar solvents as ethanol or water although with reverse results. In water, the *anti* isomer is formed preferential (15:85) and in ethanol the *syn* selectivity prevails in 70:30 (Table 1, entries 2 and 6). Interestingly, excellent yield of corresponding  $\beta$ -amino-ketones was obtained in solvent free conditions although slightly selectivity was observed (Table 1, entry 7). Although good *anti* selectivity prevails in aqueous media the main drawback is the formation of imine as a side product, which could be due to the precipitation of these compounds in aqueous media.

Varying the amount of catalyst from 5 w% to 10 w% didn't affect the reaction yield substantially as only a 2 to 3 % rise was observed (Table 1, entry 8).

The *anti/syn* ratio was determined by  $^1\text{H}$  NMR spectroscopy, for the signals corresponding to the 4H-proton. The coupling constants for the *anti*- and *syn* isomer are around 7Hz and 4Hz respectively.

**Table 1.** Optimization of reactions conditions<sup>[a]</sup>



Entry	Catalyst	Solvent	Isolated yield (%)	Syn: anti
1	No catalyst	No solvent	trace	-----
2	Fe <sub>3</sub> O <sub>4</sub> -Cys <sup>b</sup>	H <sub>2</sub> O	75	15:85
3	Fe <sub>3</sub> O <sub>4</sub> -Cys	CH <sub>3</sub> CN	58	40:60
4	Fe <sub>3</sub> O <sub>4</sub> -Cys	CH <sub>3</sub> COOEt	62	54:46
5	Fe <sub>3</sub> O <sub>4</sub> -Cys	MeOH	60	43:57
6	Fe <sub>3</sub> O <sub>4</sub> -Cys	EtOH	55	70:30
7	Fe <sub>3</sub> O <sub>4</sub> -Cys	No solvent	93	45:55
8	Fe <sub>3</sub> O <sub>4</sub> -Cys	No solvent	95 <sup>c</sup>	45:55
9	Cysteine <sup>d</sup>	No solvent	40	-----
10	Fe <sub>3</sub> O <sub>4</sub>	No solvent	Trace	-----

<sup>[a]</sup> **Reaction conditions:** Aldehyde **5** (5 mmol), arylamine **4** (5 mmol), cyclohexanone **6** (10 mmol), Fe<sub>3</sub>O<sub>4</sub>-Cys **2**, 5 wt% respectively to aldehyde, time (2 h), room temperature (22 °C). <sup>[b]</sup>20 % yield of imine as side product; <sup>[c]</sup>10 wt% of catalyst used. <sup>[d]</sup>No reusability of cysteine.

2-(Phenyl(phenylamino)methyl)cyclohexanone (**3a**): solid obtained in 93 % yield, mp 138-139°C (lit<sup>1</sup> 138-139°C); <sup>1</sup>H NMR (400 MHz, CDCl<sub>3</sub>) δ: 7.37 -7.18 (m, 5H), 7.07 – 7.03 (m, 2H), 6.65– 6.60 (m, 1H), 6.55 – 6.51 (t, 2H, *J*=7 Hz), 4.80 (d, *J*=3.8, 0.45 H<sub>syn</sub>), 4.63 (d, *J*=6.9, 0.55 H<sub>anti</sub>), 2.80-2.74 (m, 1H), 2.43-2.32 (m, 2H), 2.04-1.59 (m, 6H).

2-[(4-Bromophenyl)(phenylamino)methyl)cyclohexanone (**3b**) obtained in 91 % yield, mp 109-110°C (lit<sup>2</sup> 110-112°C); <sup>1</sup>H NMR (400 MHz, CDCl<sub>3</sub>) δ: 7.41 (d, 2H, *J* = 6.8 Hz), 7.26 – 7.25 (m, 2H), 7.15 – 7.06 (m, 2H), 6.65 – 6.64 (m, 1H), 6.50 (d, 1H, *J* = 6.7 Hz), 4.72 (m, 0.53 H<sub>syn</sub>), 4.57 (d, 0.47 H<sub>anti</sub>, *J* = 5.4 Hz), 2.74 (m, 1H), 2.54-2.33 (m, 2H), 2.04-1.59 (m, 6H).

2-[(4-Chlorophenyl)(phenylamino)methyl]cyclohexanone (**3c**) obtained in 90% yield; mp 137-138°C (lit<sup>1c, 2a</sup> 137-138 °C); <sup>1</sup>H NMR (400 MHz, CDCl<sub>3</sub>) δ: 7.32-7.26 (m, 4H), 7.17-7.06 (m, 2H), 6.65 (d, 1H, *J* = 6.8 Hz), 6.50-6.49 (m, 2H), 4.74 (m, 0.43H), 4.59 (d, 0.57H, *J* = 5.8 Hz), 2.73 (m, 1H), 2.54-2.32 (m, 2H), 2.04-1.59 (m, 4H).

2-(((4-Chlorophenyl)amino)(phenyl)methyl)cyclohexanone (**3d**) obtained in 92% yield; mp 135-136°C (lit<sup>3</sup> 136-137°C); <sup>1</sup>H NMR (400 MHz, CDCl<sub>3</sub>) δ: 7.39-7.21 (m, 5H), 7.00-6.99 (m, 2H), 6.45 (d, 2H, *J* = 5.5 Hz), 4.74 (m, 0.49 H), 4.54 (d, 0.51 H, *J* = 6.2 Hz), 2.7(m, 1H), 2.43-2.33 (m, 2H), 2.02-1.41(m, 6H).

2-(Phenyl(*p*-tolylamino)methyl)cyclohexanone (**3e**) obtained in 92 % yield; mp 116-117°C (lit<sup>1c, 4</sup> 116-118°C); <sup>1</sup>H NMR (400 MHz, CDCl<sub>3</sub>) δ: 7.35-7.20 (m, 5H), 6.88-6.86 (d, 2H, *J* = 6.2 Hz), 6.4-6.46 (m, 2H, *J* = 5.2 Hz), 4.76 (m, 0.4 H), 4.58 (d, 0.6 H, *J* = 6.9 Hz), 2.7 (m, 1H), 2.43-2.34 (m, 2H), 2.34 (s, 3H), 2.03-1.57(m, 6H).

2-((4-Methoxyphenyl)(phenylamino)methyl)cyclohexanone (**3f**)<sup>5</sup> obtained in 89 % yield; <sup>1</sup>H NMR (400 MHz, CDCl<sub>3</sub>) δ: 7.29-7.25(m, 3H), 7.06 (m, 2H), 6.83-6.82 (m, 2H), 6.75-6.54 (m, 3H), 4.71 (m, 0.32 H), 4.57 (d, 0.68 H, *J* = 6.6 Hz), 3.76 (s, 3H), 2.75(m, 1H), 2.42-2.33 (m, 2H), 2.04-1.57 (m, 6H).

2-(((3-Chlorophenyl)amino)(phenyl)methyl)cyclohexanone (**3g**) obtained in 93 % yield; mp 121-122°C (lit<sup>3b, 6</sup> 122-123°C); <sup>1</sup>H NMR (400 MHz, CDCl<sub>3</sub>) δ: 7.38-7.23 (m, 5H), 6.99 – 6.95 (m, 1H), 6.66-6.42 (m, 3H), 4.77 (d, 0.42 H, *J* = 3.8 Hz), 4.55 (d, 0.58 H, *J* = 6.8 Hz), 2.89-2.81(m, 1H), 2.43-2.19 (m, 2H), 2.04-1.58 (m, 6H).

### Synthesis of hexahydroquinoline derivative (7)

**Ethyl 4-(3,4-bis(benzyloxy)phenyl)-2,7,7-trimethyl-5-oxo-1,4,5,6,7,8-hexahydro-quinoline-3-carboxylate 7:** A solution of 3,4-diphenoxy benzaldehyde (5.0 mmol), ammonium acetate (10 mmol), ethyl acetoacetate (5 mmol), 5,5-dimethylcyclohexane-1,3-dione aldehyde (5 mmol) and Fe<sub>3</sub>O<sub>4</sub>-Cys (5 wt % respectively to aldehyde) in ethanol (3 mL) was stirred at room temperature for 25 min. After terminus of the reaction monitored by TLC (n-hexane and ethyl acetate; 70:30), the catalyst was separated magnetically. To the solution was added ethyl acetate (10 mL). The organic layer was washed with saturated NaHCO<sub>3</sub> (aq) and brine, dried with anhydrous Na<sub>2</sub>SO<sub>4</sub>, and concentrated to dryness. The crude mixture was purified by crystallization in ethanol and the hydroquinoline **7** was obtained in 88% yield: IR(KBr)  $\nu_{\max}$ : 3284, 3206, 1694, 1640, 1605 cm<sup>-1</sup>; <sup>1</sup>H NMR (400 MHz, CDCl<sub>3</sub>) δ: 7.42-7.28 (m, 10H, PhH), 6.90 (s, 1H, ArH2), 6.80 (d, 1H, ArH5/6), 6.77 (d, 1H, ArH5/6), 5.87 (bs, 1H, NH), 5.08 (d, 4H, OCH<sub>2</sub>Ph), 4.96 (s, 1H, H4), 4.01 (q, 2H, OCH<sub>2</sub>CH<sub>3</sub>), 2.31 (s, 3H, CH<sub>3</sub>), 2.28-2.05 (m, 4H, CH<sub>2</sub>, CH<sub>2</sub>), 1.17 (t, 3H, OCH<sub>2</sub>CH<sub>3</sub>), 1.05 (s, 3H, CH<sub>3</sub>), 0.90 (s, 3H, CH<sub>3</sub>); <sup>13</sup>C NMR δ: 14.23 (CH<sub>3</sub>), 19.4 (CH<sub>3</sub>), 27.2 (CH<sub>3</sub>), 29.3 (CH<sub>3</sub>), 31.8 (C7),

35.6 (C4), 41.0 (C6/8), 50.45 (C6/8), 59.8 (OCH<sub>2</sub>), 71.36 (OCH<sub>2</sub>), 106.3 (C10), 112.05 (C3), 114.5 (ArC5), 115.36 (ArC2), 120.9 (ArC6), 127.3 (Ph), 127.5 (Ph), 127.6 (Ph), 128.4 (Ph), 137.6 (Ph), 137.8 (Ph), 140.5 (C2), 142.9 (C9), 147.3 (ArC4), 148.4 (ArC3), 167.3 (CO), 195.4 (CO); MSEI(+) m/z: 551 [M]<sup>+</sup>, 262 [M-PhCH<sub>2</sub>O)<sub>2</sub>C<sub>6</sub>H<sub>3</sub>]<sup>+</sup>, 91 [C<sub>7</sub>H<sub>7</sub>]<sup>+</sup>. HRMSEI(+) calcd for C<sub>35</sub>H<sub>37</sub>NO<sub>5</sub> [M]<sup>+</sup> 551.2672 found 551.2668.

### FT-IR of Ferrite, L-Cysteine and Ferrite-Cys

The infrared spectra of Fe<sub>3</sub>O<sub>4</sub>-L-cysteine are depicted in Figure 1 in comparison with those of Fe<sub>3</sub>O<sub>4</sub>, and L-cysteine. A broad band observed at 2500-3300 cm<sup>-1</sup>, confirms the stretching of the OH group, from the COOH group of cysteine as also the band at 1620 cm<sup>-1</sup> related to the carbonyl group of the same functionality which clearly indicates the presence of cysteine over ferrite surface.

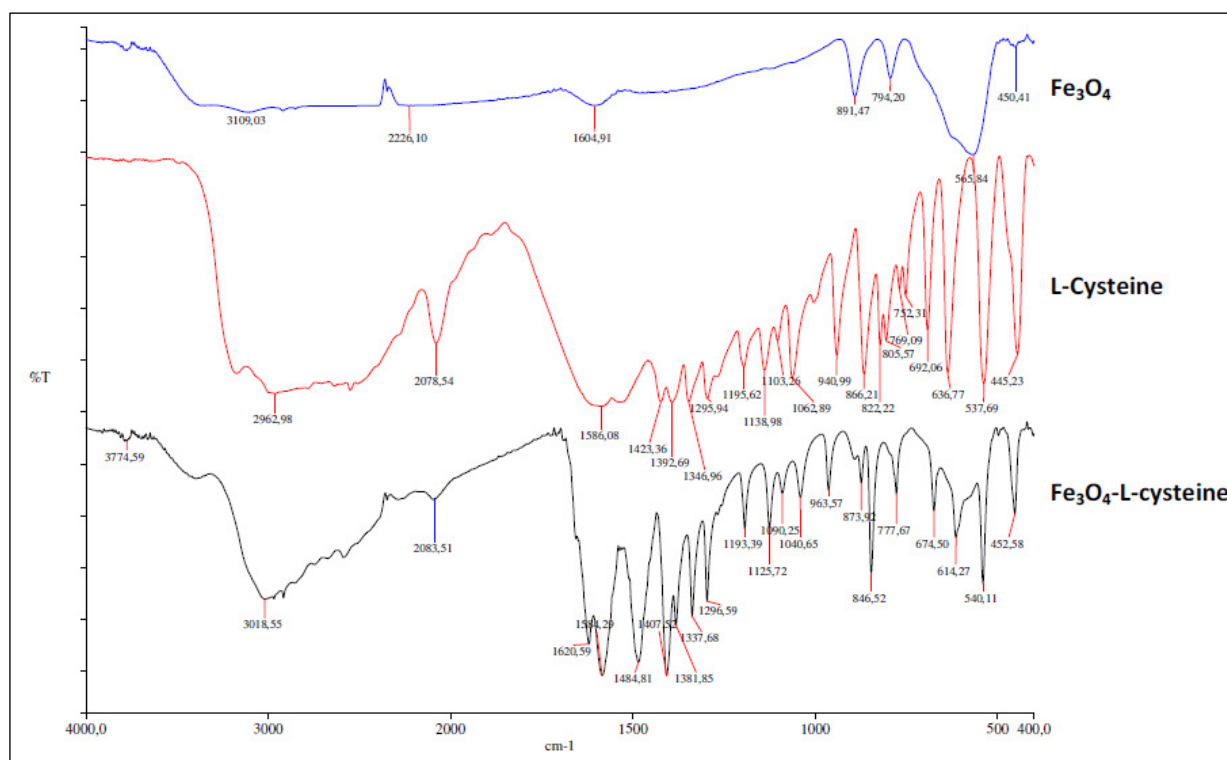


**Figure 1.** FT Infrared spectrum of Fe<sub>3</sub>O<sub>4</sub>, L-Cysteine and Fe<sub>3</sub>O<sub>4</sub>-Cys (KBR)

## TOF-SIMS analysis of Ferrite-Cys

To confirm the presence of cysteine over the surface of ferrite, we have characterized catalyst with TOF-SIMS. The catalyst sample was analyzed in both positive and negative TOF-SIMS static mode, which means that we kept the total primary ion dose of  $\text{Ga}^+$  well below the static limit of  $1 \times 10^{13}$  ions /  $\text{cm}^2$ . Figure 2 shows the mass spectra in the  $m/z$  range of 0-250. In positive mode, diagnostic ions of cysteine (cySH) observed at  $m/z$  241, 152, 122, 120, 74, 43, and 18, corresponds to  $[\text{cySScy}+\text{H}]^+$ ,  $[\text{cySS}]^+$ , protonated cysteine  $[\text{cySH}+\text{H}]^+$ , deprotonated cysteine ion  $[\text{cyS}]^+$ ,  $[\text{cyS}-\text{CO}_2\text{H}_2]^+$ ,  $[\text{H}_2\text{NCHCH}_2]^+$ , and ammonium protonated molecule  $[\text{NH}_4]^+$ , respectively. It is interesting to note that all assigned fragments mentioned here except the two fragments ions at  $m/z$  43 and  $m/z$  18 corresponding to those observed by Rubino *et al.*<sup>7</sup> who studied cysteine containing amino acids using electrospray ionization. It can be seen that spectrum is rich in ion fragments correspond to cysteine with dominant cysteine fragment  $[\text{H}_2\text{NCHCH}_2]^+$ , and distinct peaks of ferrite observed at  $m/z$  56  $[\text{Fe}]^+$ , and 73  $[\text{FeOH}]^+$ . The most interesting ion peak that might be due to attachment of cysteine with ferrite is obvious at  $m/z$  130  $[\text{Fe}+\text{cy}-\text{CH}_2]^+$ . In negative ion mode, characteristic fragment ions of cysteine above  $m/z$  100 observed at  $m/z$  239, 152, 120, 105, and 105, correspond to dimer cysteine ion  $[\text{cySScy}-\text{H}]^+$ , sulfur adduct ion  $[\text{cySS}]^-$ , deprotonated cysteine  $[\text{cyS}]^-$ , a fragment by losing ammonia  $[\text{cySH}-\text{NH}_2]^-$ , and  $[\text{cySH}-\text{OH}]^-$ , respectively. The characteristic ions of cysteine below  $m/z$  100 are mainly sulfur, sulfur oxides and cyanide ions as shown in Figure 2b. From the SIMS results one can conclude that cysteine is present on the surface of the ferrite. The unchanged molecular structure of cysteine is also revealed from these results.



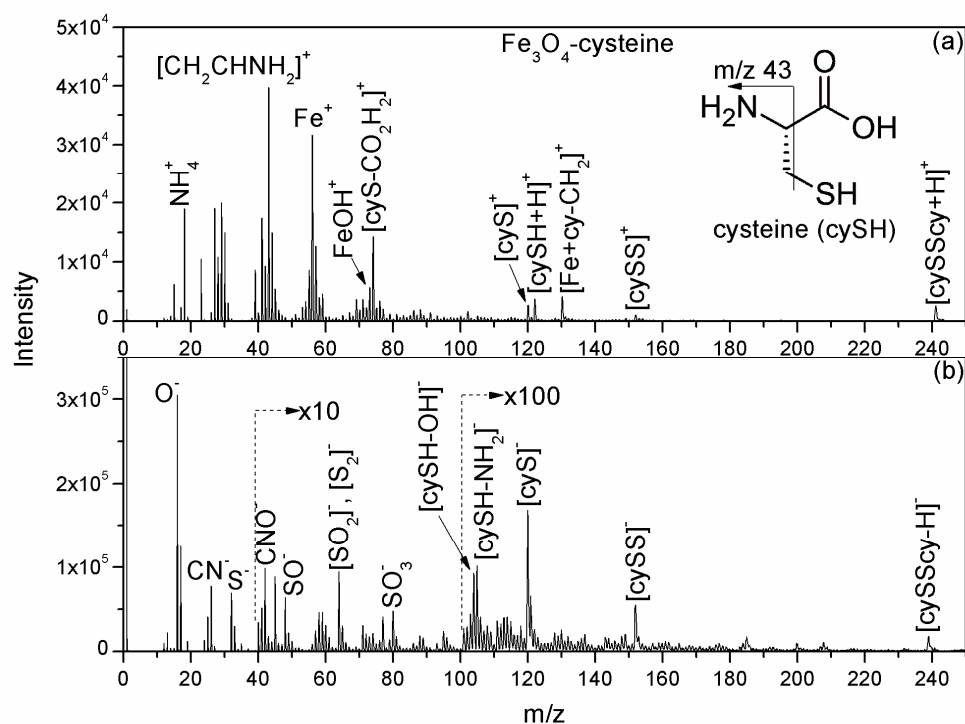


**Figure 2.** Positive (a) and negative (b) TOF-SIMS from  $\text{Fe}_3\text{O}_4$ -Cys analyzed with upgraded VG Ionex 1X23S, equipped with a  $\text{Ga}^+$  liquid metal ion gun. Molecular structure of cysteine is abbreviated as cySH for structurally assigning the molecular ion peaks.

### Field-emission gun scanning electron microscope (FEG-SEM)

From analysis of FEG-SEM images using a 25kV acceleration voltage, uniform-sized magnetic nanoparticles with somewhat spherical morphology and a marked tendency to form large clusters were observed (Figure 3a and b). This tendency is not surprising, given the MNPs small size and magnetic characteristics.

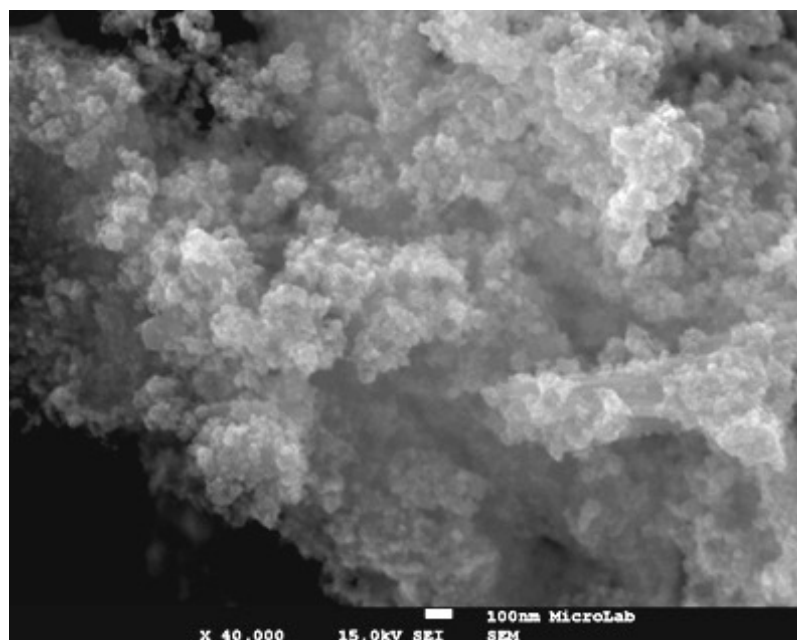


**Figure 3 a)** SEM images of  $\text{Fe}_3\text{O}_4\text{-Cys 2}$  at 100 nm.

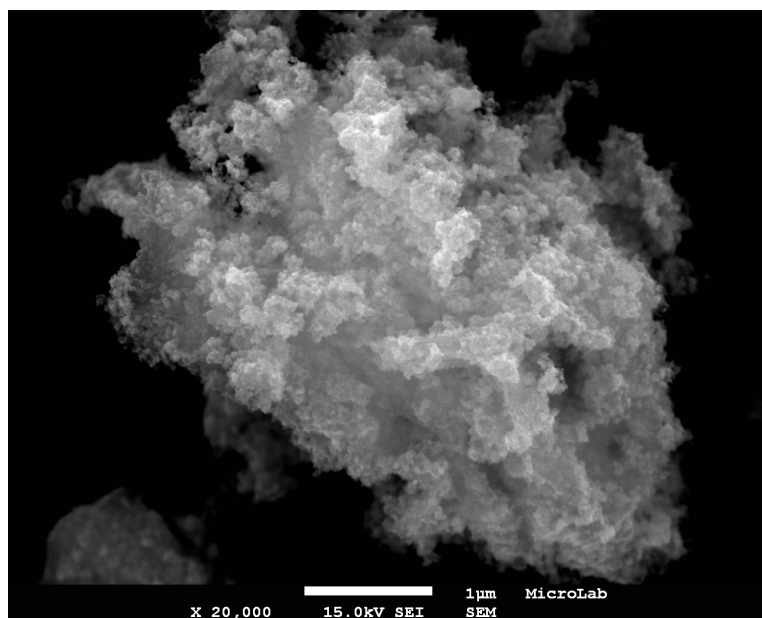


**Figure 3 b)** SEM images of  $\text{Fe}_3\text{O}_4\text{-Cys 2}$  at 1  $\mu\text{m}$ .

### Transmission electron microscopy (TEM) of Ferrite-Cys

Transmission electron microscopy (TEM) experiments were performed on a Hitachi H8100 microscope, with a ThermoNoran light elements EDS detector and a CCD camera for image acquisition. The TEM images of  $\text{Fe}_3\text{O}_4\text{-Cys}$  at 100 nm and 200 nm and a histogram based on the TEM measurements was established, showing a size distribution in agreement with the XRD indications (Figure 4 a-c).

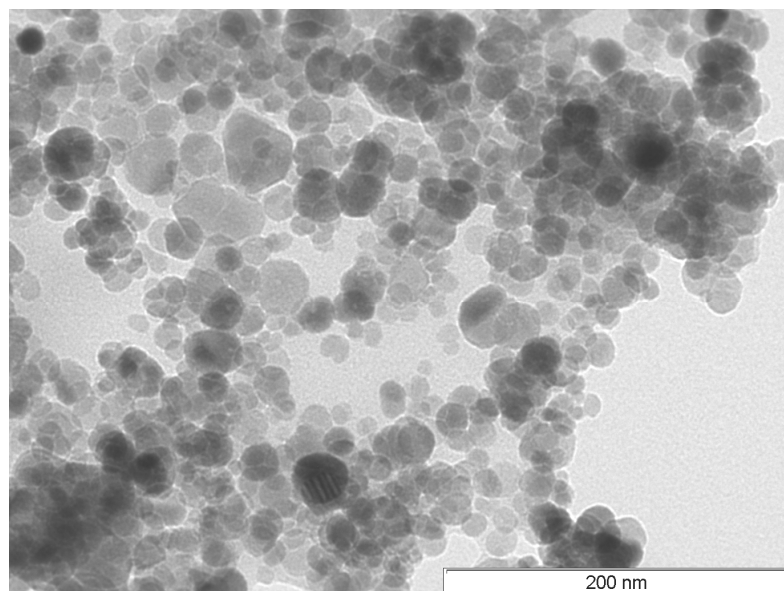


**Figure 4 a)** TEM images of Fe-Cys at 200 nm.

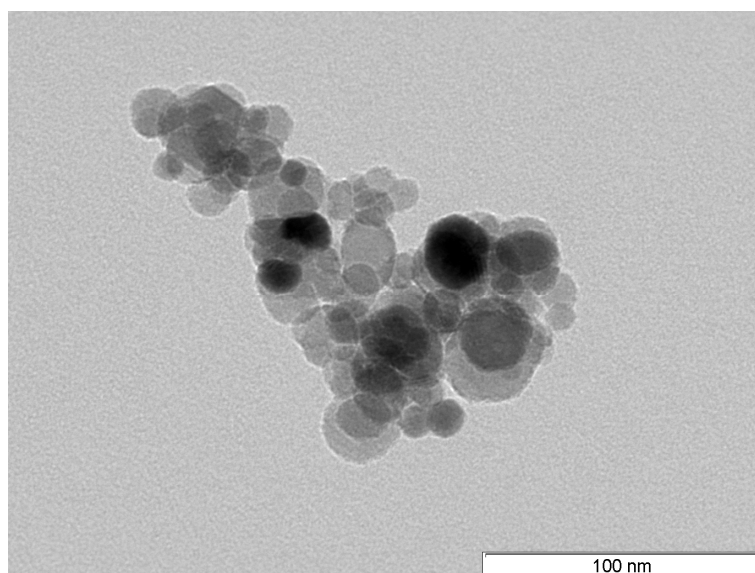


**Figure 4 a)** TEM images of Fe-Cys at 100 nm.

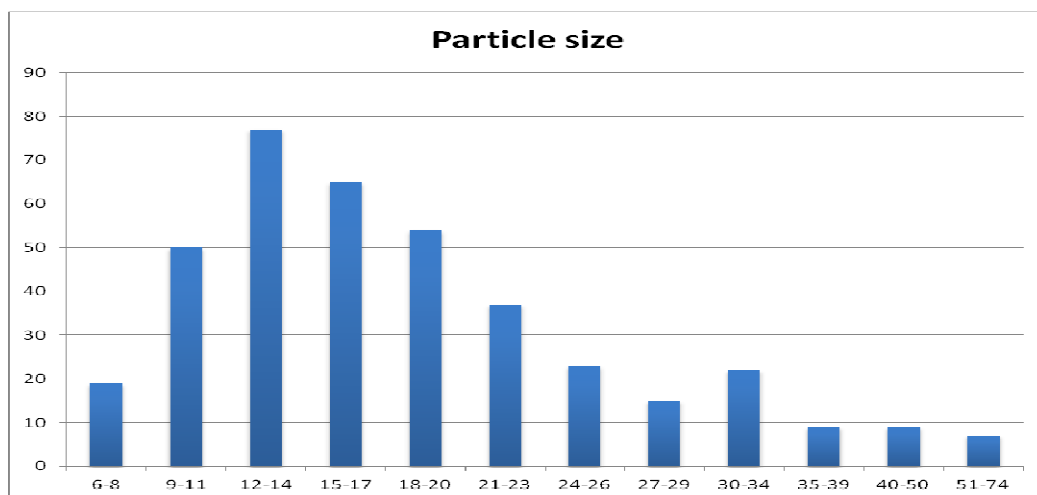


Figure 4. c) Histogram of  $\text{Fe}_3\text{O}_4$ -Cys showing particle size distribution

## Stability of Ferrite-Cys

### Reusability experimental procedure

The stability of  $\text{Fe}_3\text{O}_4\text{-Cys}$  was tested on the reaction with benzaldehyde, aniline and cyclohexanone by recycling and reuse of the catalyst nine times without any significant loss of the catalytic activity (Figure 5). After completion of the reaction, monitored by thin layer chromatography, ethyl acetate was added to the reaction mixture which was then decanted using an external magnet. The  $\text{Fe}_3\text{O}_4\text{-Cys}$  catalyst was washed with methanol (3 X 5 mL) and dried at 60 °C for 2 h. To the flask was subsequently added new reagents following the reported conditions.

After each cycle  $\text{Fe}_3\text{O}_4\text{-Cys}$  MNPs were separated by simple magnet and used for next cycle. Also the morphology of  $\text{Fe}_3\text{O}_4\text{-Cys}$  after nine consecutive cycles of reactions was verified by TEM. Slightly changes in morphology of particles were observed, and a significant increase in the drive for particle clustering is clearly discernible. (Figure 6 a, b).

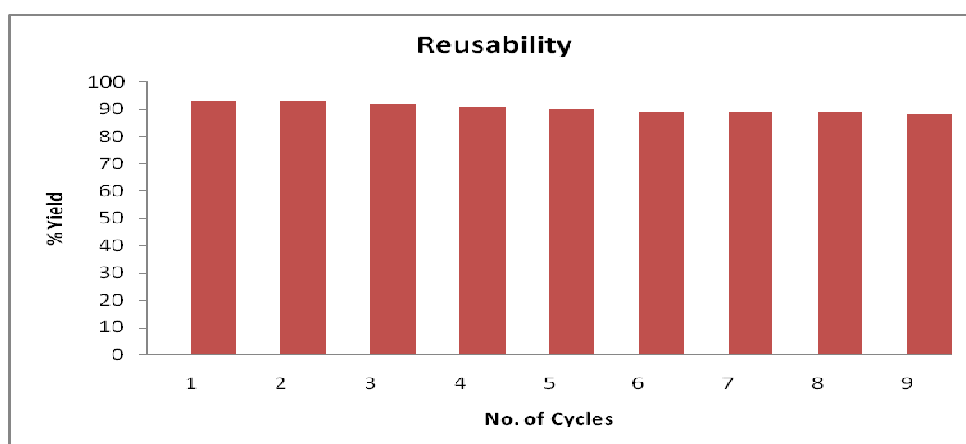


**Figure 5.** Reusability profile of  $\text{Fe}_3\text{O}_4\text{-Cys}$

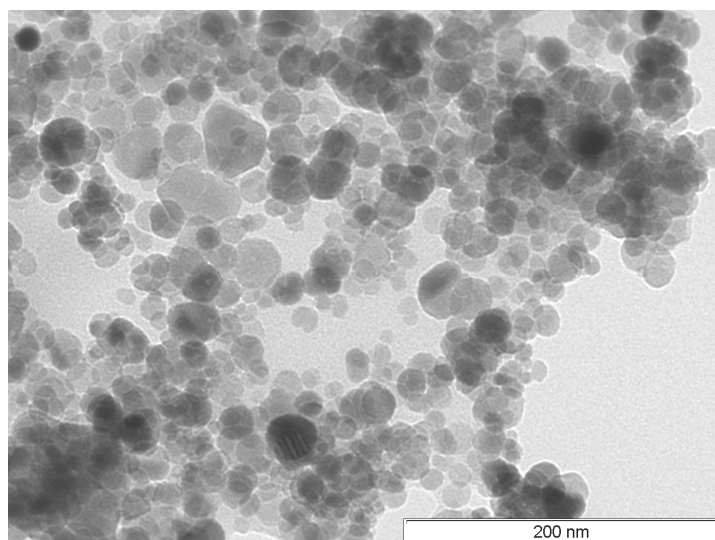


**Figure 6.** a) TEM  $\text{Fe}_3\text{O}_4\text{-Cys}$  at 200 nm.

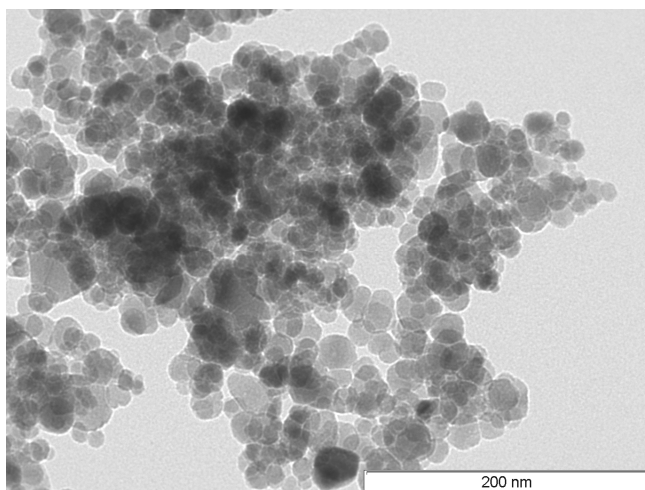
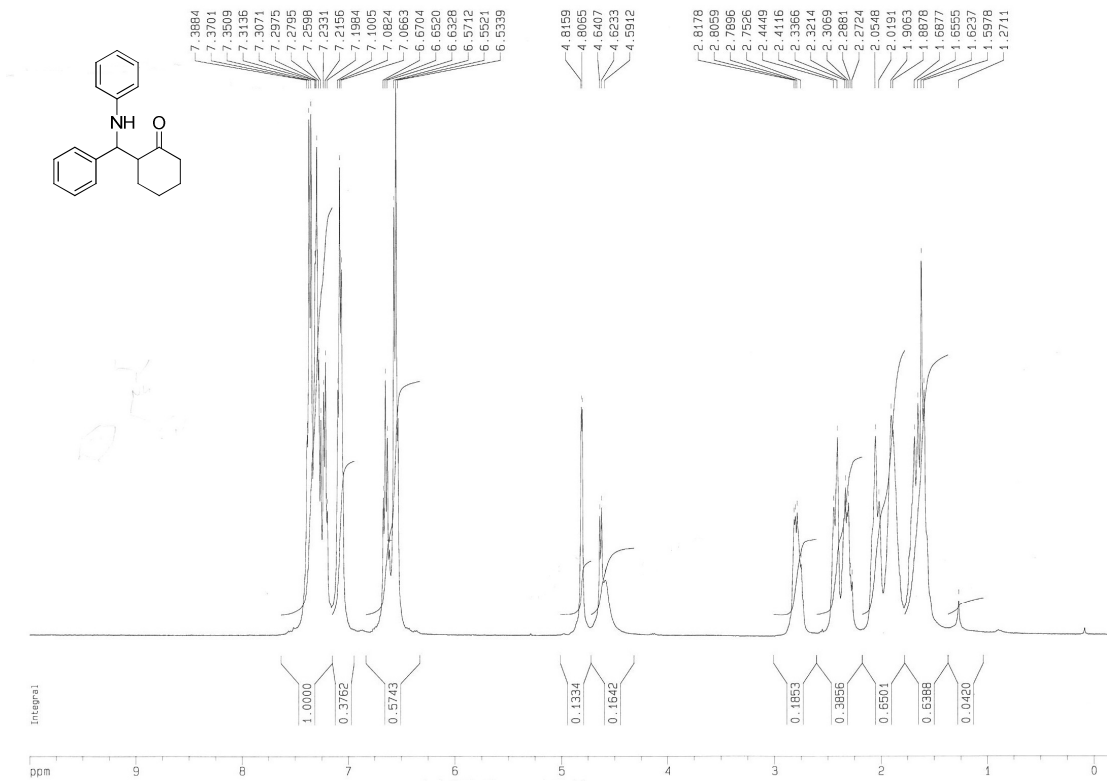


**Figure 6.** b) TEM of reused  $\text{Fe}_3\text{O}_4\text{-Cys}$  after 9 cycle at 200 nm.

## References

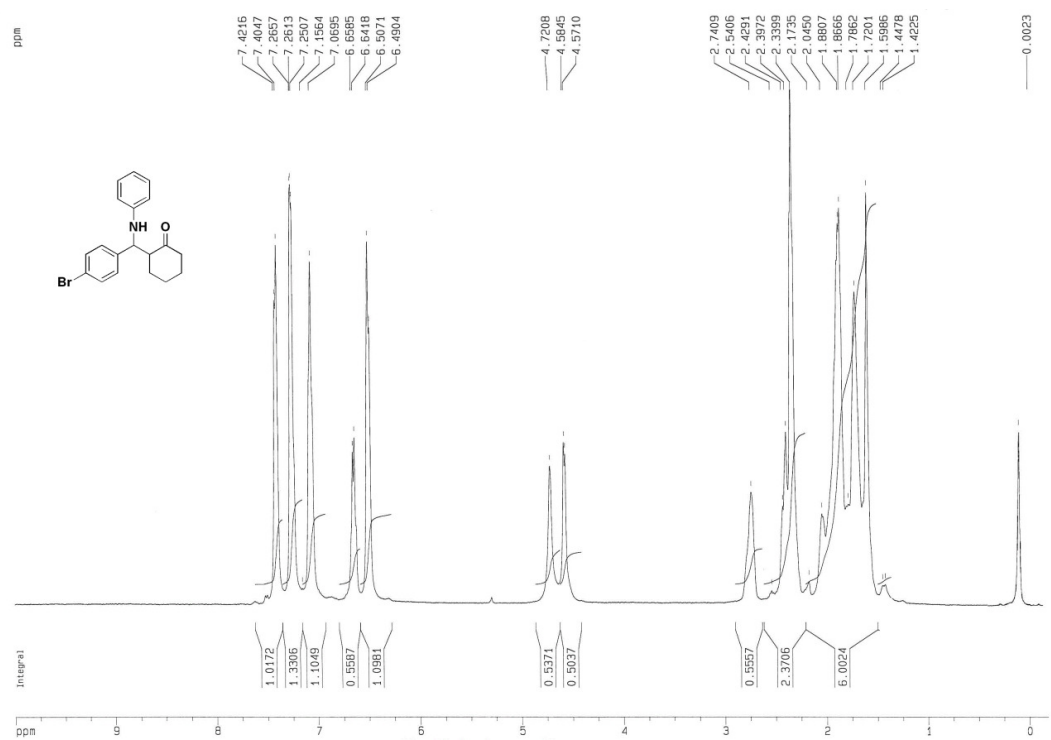
- 1 (a) S. Kobayashi and S. Nagayama, *J. Org. Chem.*, 1997, **62**, 232-233; (b) H. Wu, X. M. Chen, Y. Wan, L. Ye, H. Q. Xin, H. H. Xu, C. H. Yue, L. L. Pang, R. Ma and D. Q. Shi, *Tet. Lett.*, 2009, **50**, 1062-1065; (c) W. B. Yi and C. Cai, *J. Fluor. Chem.*, 2006, **127**, 1515-1521.
- 2 (a) Q. X. Guo, H. Liu, C. Guo, S. W. Luo, Y. Gu and L. Z. Gong, *J. Am. Chem. Soc.*, 2007, **129**, 3790-+; (b) M. A. Bigdeli, F. Nematì and G. H. Mahdavinia, *Tet. Lett.*, 2007, **48**, 6801-6804.
- 3 (a) K. Manabe and S. Kobayashi, *Org. Lett.*, 1999, **1**, 1965-1967; (b) A. R. Massah, R. J. Kalbasi and N. Samah, *Bull. Korean Chem. Soc.*, 2011, **32**, 1703-1708.
- 4 P. Goswami and B. Das, *Tet. Lett.*, 2009, **50**, 2384-2388.
- 5 T. Ollevier, E. Nadeau and A.-A. Guay-Begin, *Tet. Lett.*, 2006, **47**, 8351-8354.
- 6 H. Wu, Y. Shen, L. Y. Fan, Y. Wan, P. Zhang, C. F. Chen and W. X. Wang, *Tetrahedron*, 2007, **63**, 2404-2408.
- 7 F. M. Rubino, C. Verduci, R. Giampiccolo, S. Pulvirenti, G. Brambilla and A. Colombi, *J. Mass Spectrom.*, 2004, **39**, 1408-1416.

Spectrum of Compounds

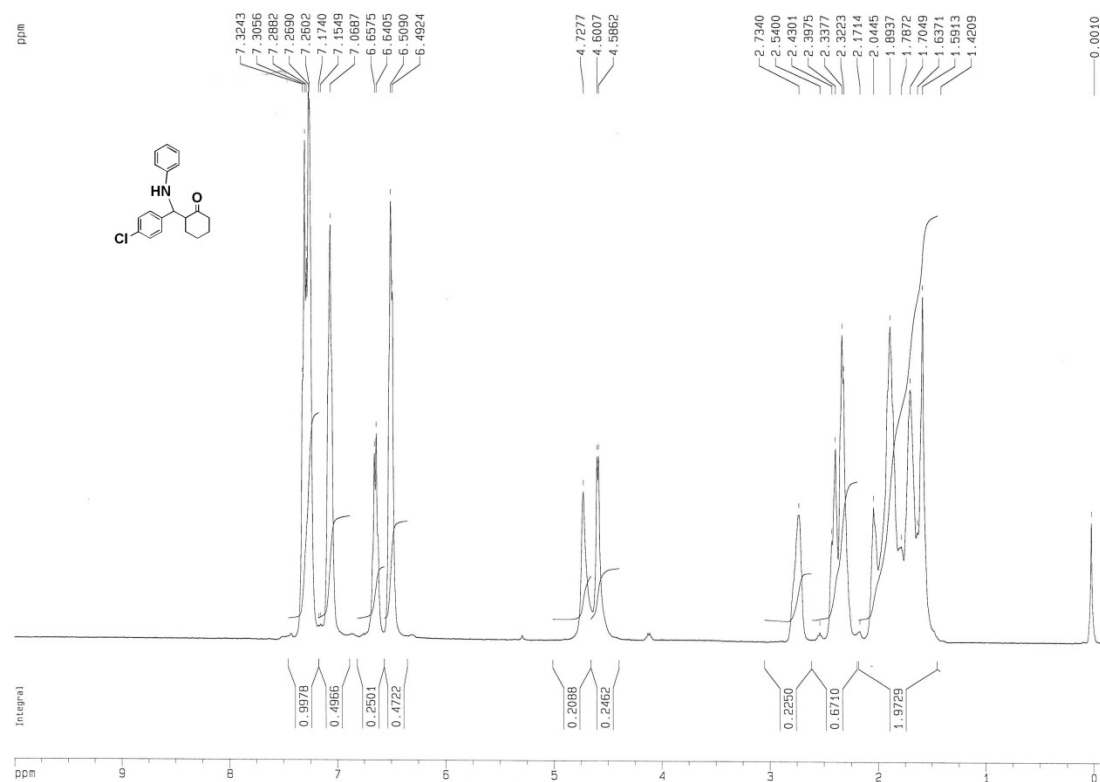


Proton NMR spectra of 2-(phenyl(phenylamino)methyl)cyclohexanone (**3a**) from thereaction in ethanol.

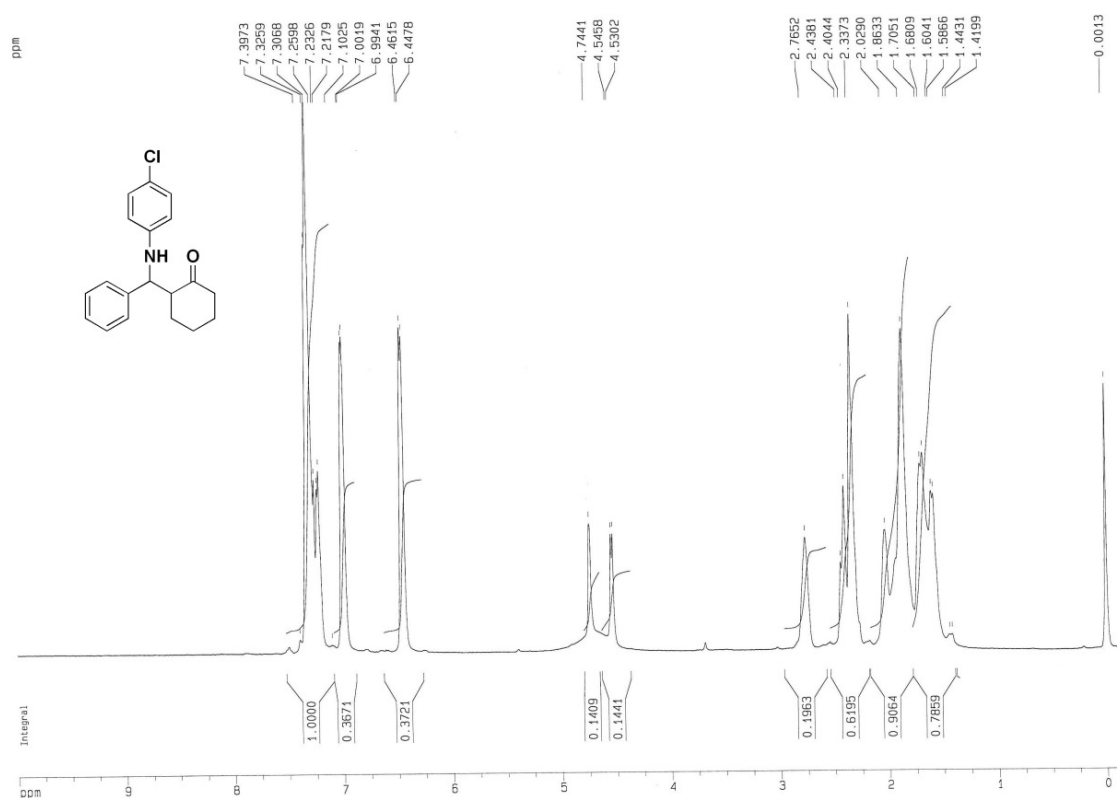




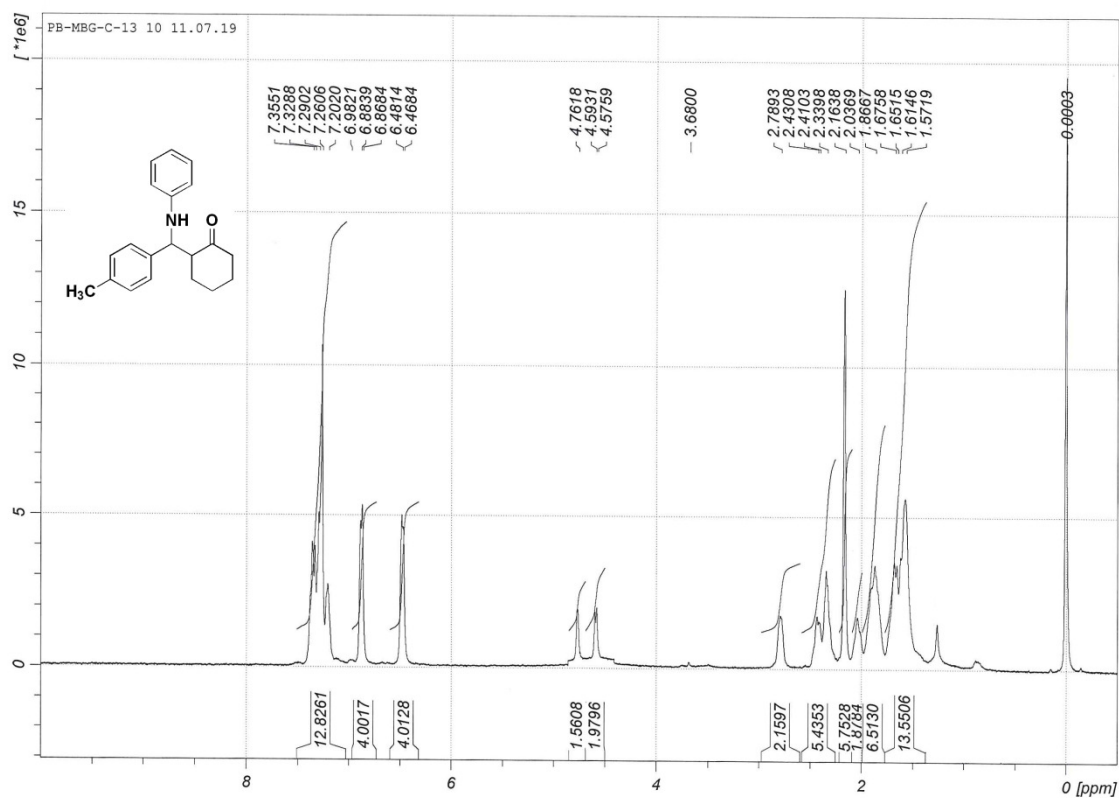
Proton NMR spectra of 2-((4-bromophenyl)(phenylamino)methyl)cyclohexanone (**3b**) in solvent free conditions.



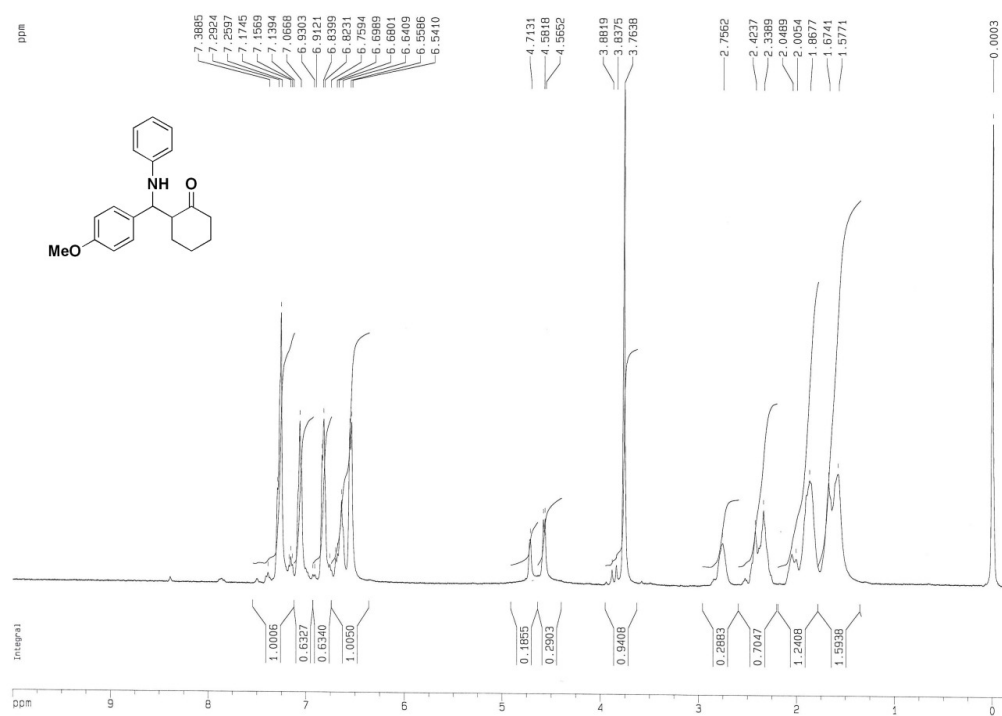
Proton NMR spectra of 2-((4-chlorophenyl)(phenylamino)methyl)cyclohexanone (**3c**) in solvent free conditions.



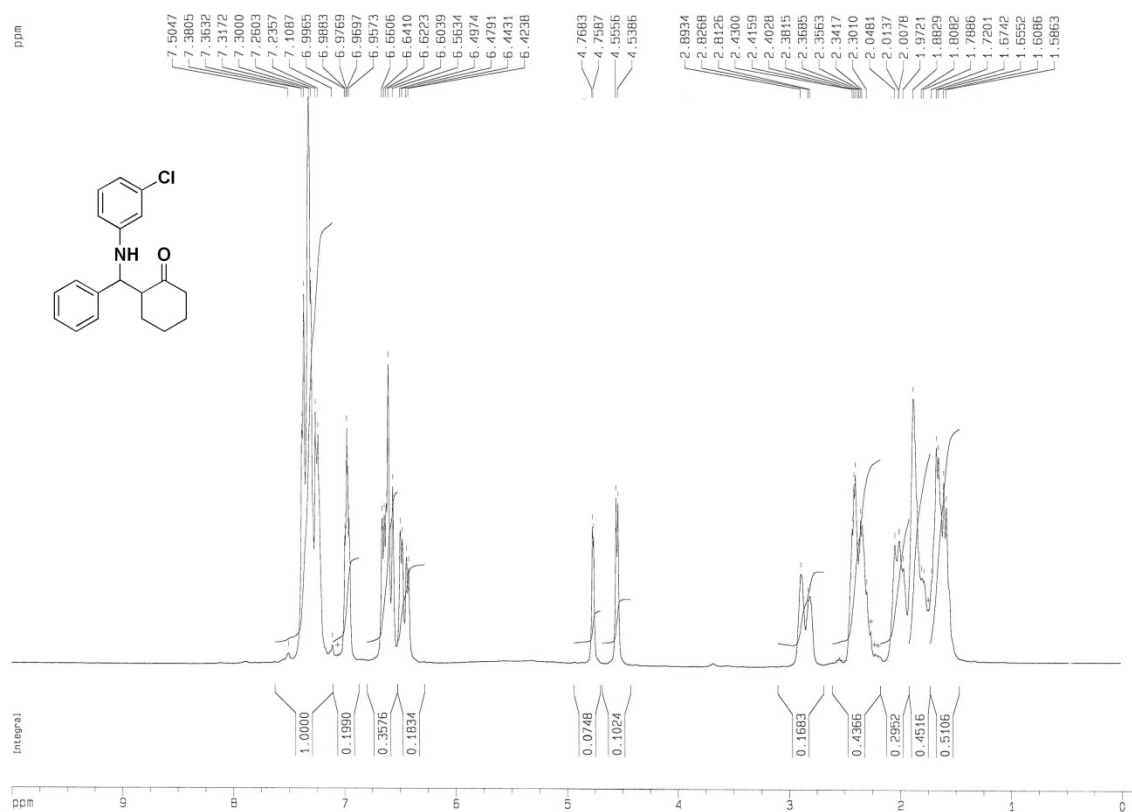
Proton NMR spectra of 2-(((4-chlorophenyl)amino)(phenyl)methyl)- cyclohexanone (**3d**) in solvent free conditions.



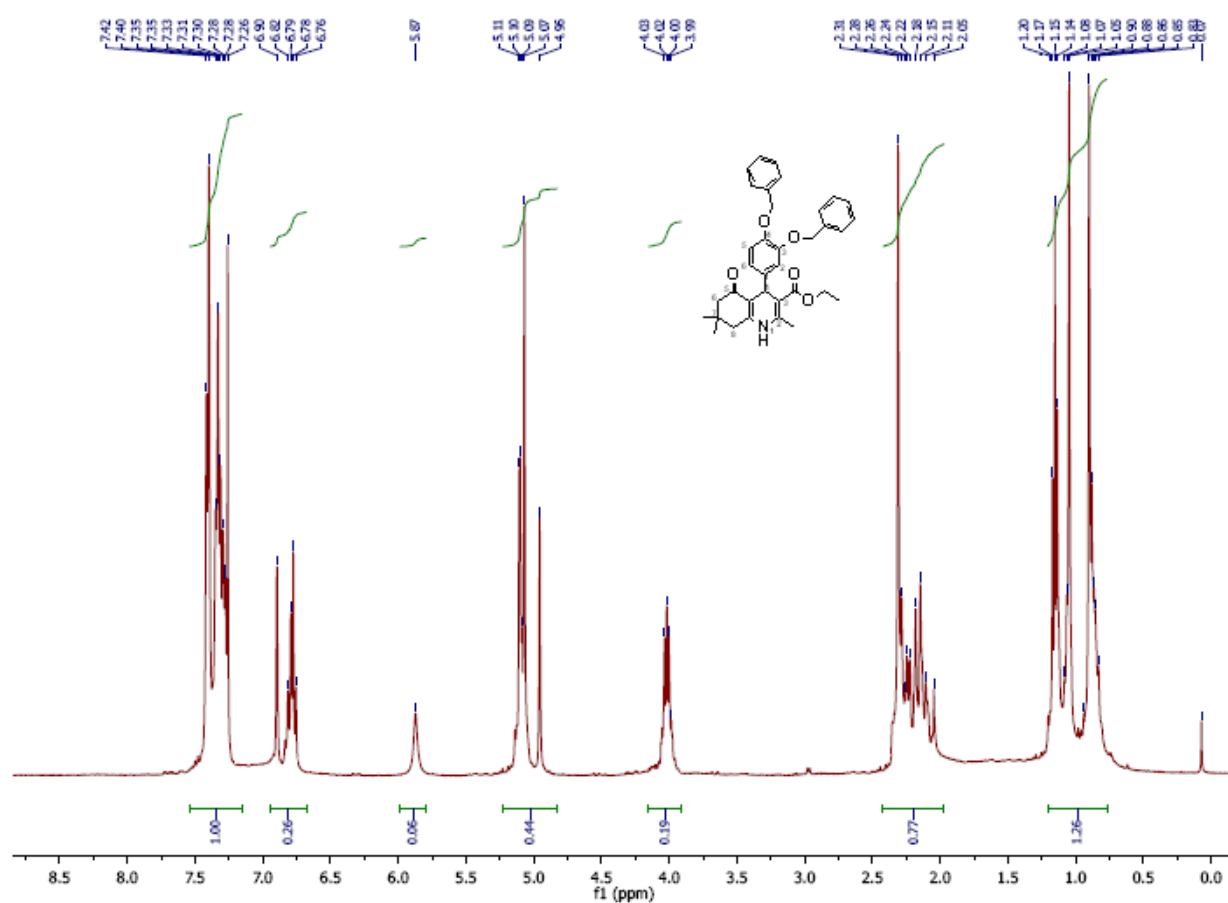
Proton NMR spectra of 2-(phenyl(p-tolylamino)methyl)cyclohexanone (**3e**) in solvent free conditions.



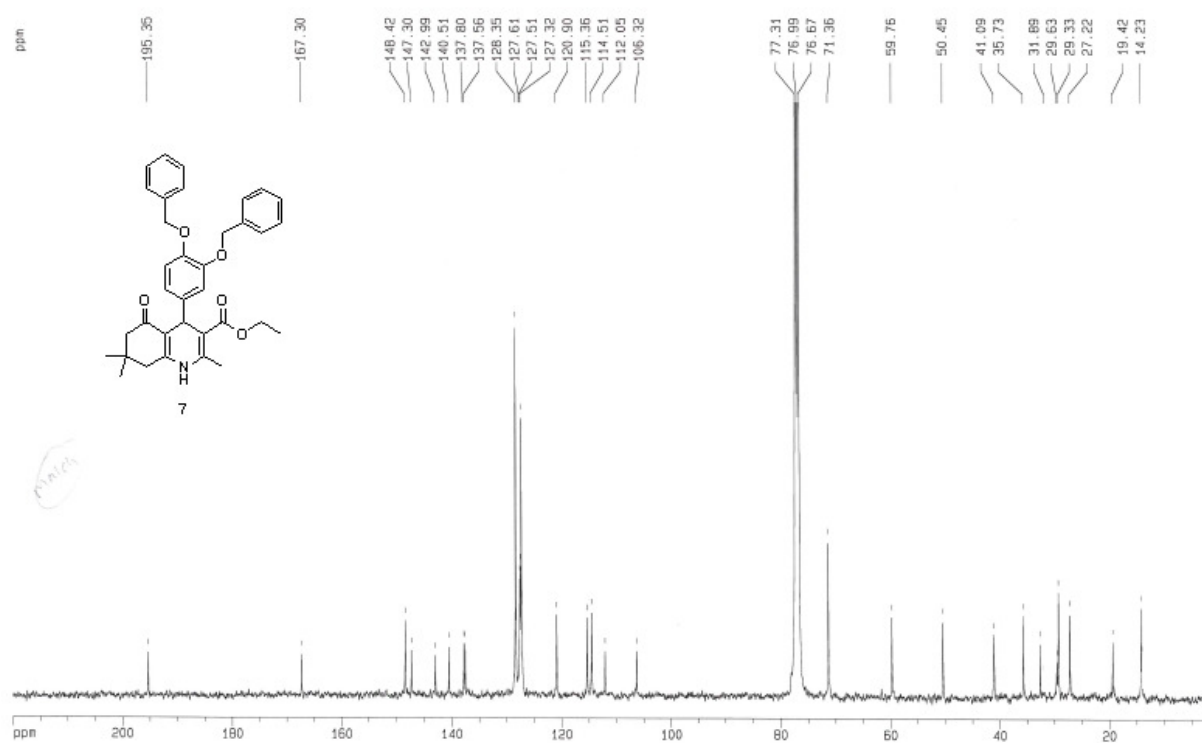
Proton NMR spectra of 2-((4-methoxyphenyl)(phenylamino)methyl)cyclohexanone (3f) in solvent free conditions.



Proton NMR spectra of 2-(((3-chlorophenyl)amino)(phenyl)methyl)cyclohexanone (**3g**) in solvent free conditions.

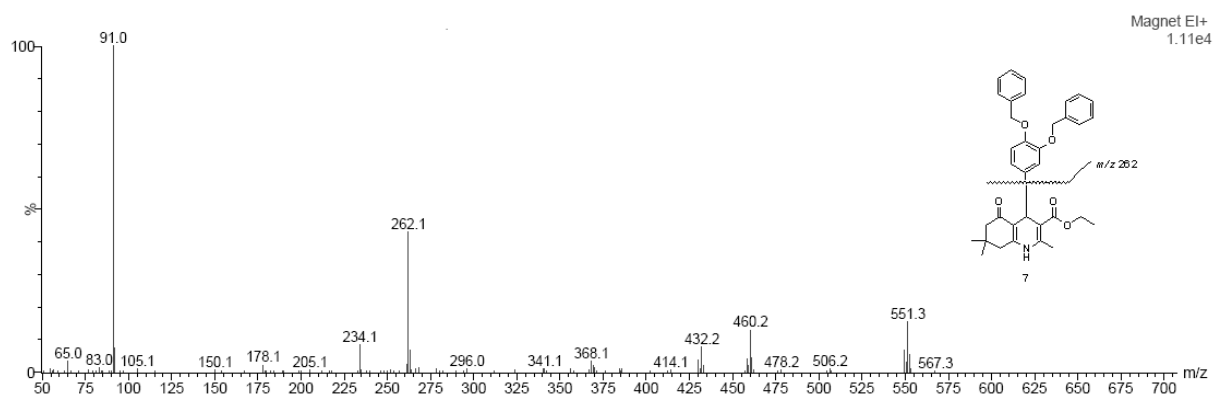


Proton NMR spectra of ethyl 4-(3,4-bis(benzyloxy)phenyl)-2,7,7-trimethyl-5-oxo-1,4,5,6,7,8-hexahydroquinoline-3-carboxylate (**7**).

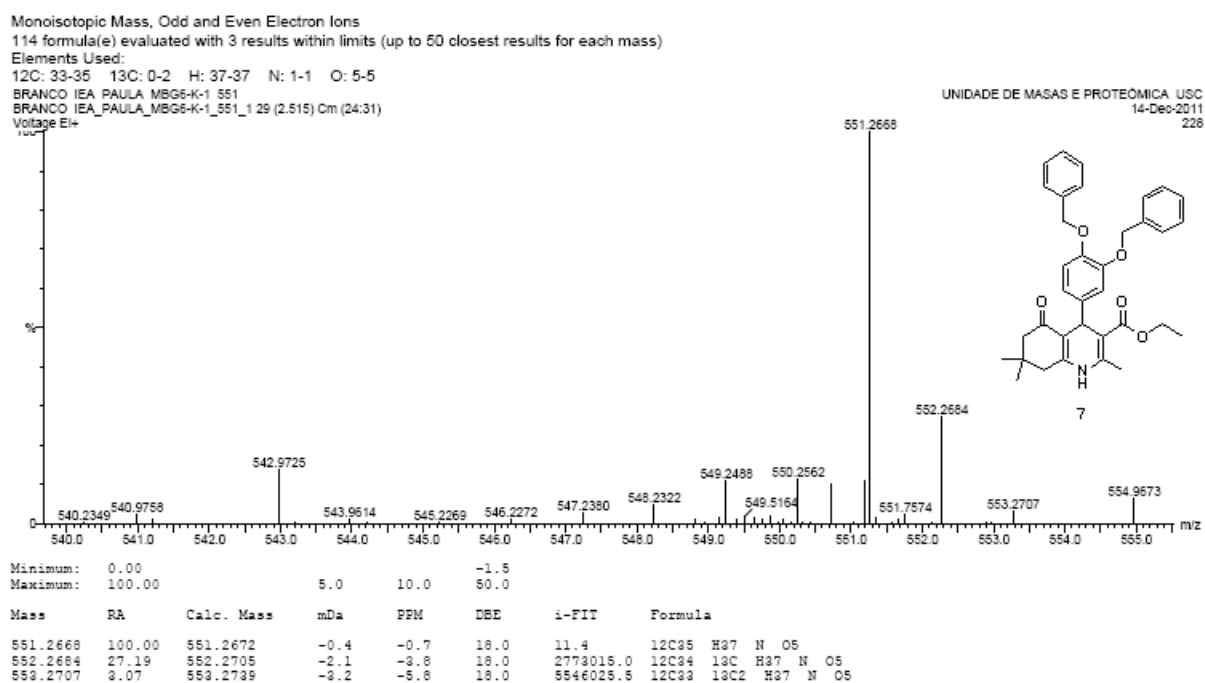


Carbon NMR spectra of ethyl 4-(3,4-bis(benzyloxy)phenyl)-2,7,7-trimethyl-5-oxo-1,4,5,6,7,8-hexahydroquinoline-3-carboxylate (**7**).





Electron impact mass spectra of ethyl 4-(3,4-bis(benzyloxy)phenyl)-2,7,7-trimethyl-5-oxo-1,4,5,6,7,8-hexahydroquinoline-3-carboxylate (**7**).



High resolution electron impact mass spectra of ethyl 4-(3,4-bis(benzyloxy)phenyl)-2,7,7-trimethyl-5-oxo-1,4,5,6,7,8-hexahydroquinoline-3-carboxylate (**7**).